THE JOURNAL OF PHYSICAL CHEMISTRY Letters

LETTER

pubs.acs.org/JPCL

Epitaxially Integrating Ferromagnetic $Fe_{1.3}Ge$ Nanowire Arrays on Few-Layer Graphene

Hana Yoon,[†] Taejoon Kang,[†] Jung Min Lee,[‡] Si-in Kim,[†] Kwanyong Seo,[†] Jaemyung Kim,[§] Won Il Park,[‡] and Bongsoo Kim*[,†]

[†]Department of Chemistry, KAIST, Daejeon 305-701

[‡]Department of Materials Science Engineering, Hanyang University, Seoul 133-791

[§]CRD Energy Lab, Samsung SDI, Gyeonggi-do, Korea

Supporting Information

ABSTRACT: We report vertical growth of ferromagnetic and metallic $Fe_{1.3}Ge$ nanowire (NW) arrays on few-layer graphene in a large area, induced by a relatively good epitaxial lattice match. Integrating well-aligned NW arrays onto graphene would offer a good opportunity to combine superb material properties of graphene with versatile properties of NWs into novel applications. $Fe_{1.3}Ge$ NWs are also synthesized on highly ordered pyrolytic graphite (HOPG). $Fe_{1.3}Ge$ NWs on graphene and HOPG show quite efficient field emission, which are ascribed to the well-interfaced vertical growth, a pointed tip, and high field-enhancement factor (β) of the NWs. The development of ferromagnetic metal NW−graphene hybrid structures would provide an important possibility to develop graphene-based spintronic, electronic, and optoelectronic devices.

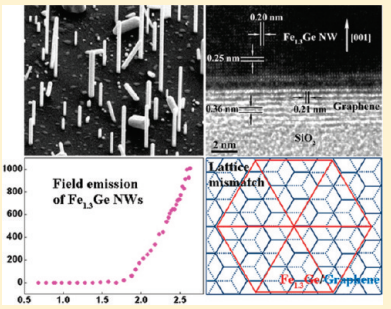

SECTION: Nanoparticles and Nanostructures

Graphene has extraordinary properties such as ultrahigh carrier mobility, large light transmission, and flexibility.[1−7] Moreover, low intrinsic spin−orbit coupling, long spin diffusion lengths, and vanishing hyperfine interaction features of graphene make it a promising medium for spin transport.[8−10] Integrating semiconducting, metallic, or ferromagnetic nanowire (NW) arrays on the graphene surface would offer a good opportunity to combine superb material properties of graphene into a greater variety of applications.[11−20] For optimum performance of the integrated devices, it is critical to have excellent contact between graphene and the NWs, especially for spin transport. To achieve an atomically well-defined interface, epitaxial integration is most desirable. Ferromagnetic metallic NWs epitaxially grown on graphene will form a solid contact between the NW and graphene, thereby allowing effective spin injection from the ferromagnetic NW to graphene. A solid interface between the NWs and graphene will also enable effective field emission (FE) of the NW emitters. Iron germanide NWs are one of the ideal materials to integrate with graphene for such advanced applications as they exhibit low resistivity and room-temperature ferromagnetism and they are compatible with existing complementary metal oxide−semiconductor (CMOS) technologies.[21−25]

Herein, we report synthesis of ferromagnetic and metallic $Fe_{1.3}Ge$ NWs vertically aligned on few-layer graphene in a large area without using any catalysts. To the best of our knowledge, this is the first report on the epitaxial growth of NWs on graphene. Because efficient spin injection and transport could be possible in the $Fe_{1.3}Ge$ NWs epitaxially grown on graphene, the NW−graphene hybrid structure can play an important role for graphene-based spintronic applications such as spin valve and spin-based logic devices.[26] We have further investigated FE properties of the $Fe_{1.3}Ge$ NWs grown on graphene for another device application. Low turn-on voltage was obtained from the $Fe_{1.3}Ge$ NW arrays grown on the graphene. To improve the cathode conductivity, we have synthesized vertical $Fe_{1.3}Ge$ NWs on HOPG, which show a very low turn-on voltage, approaching that of carbon nanotube (CNT) arrays.[16,27]

Our experimental results demonstrate that a versatile hybrid platform for three-dimensional (3D) optoelectronics and spintronics application can be fabricated by forming vertical NW arrays epitaxially aligned on few-layer graphene.

Single-crystalline hexagonal $Fe_{1.3}Ge$ NWs have been synthesized by employing a hot wall two-zone furnace having a 1 in. diameter quartz tube via a chemical vapor transport (CVT) method without using catalysts. The NWs are grown on graphene/*c*-cut sapphire substrates and graphene/SiO_2/Si substrates, all of which are made by transferring a graphene film to the substrates, and also on an HOPG substrate. Raman investigation of the graphene film after transfer revealed that the film has only a few graphene layers (Figure S1, Supporting Information).

A scanning electron microscopy (SEM) image in Figure 1a shows vertical and inclined NWs grown on the graphene/*c*-cut sapphire substrate of 5×5 mm^2. Enlarged SEM images of Figure 1b and c reveal that both the vertical and inclined $Fe_{1.3}Ge$ NWs form a

Received: March 4, 2011
Accepted: April 5, 2011

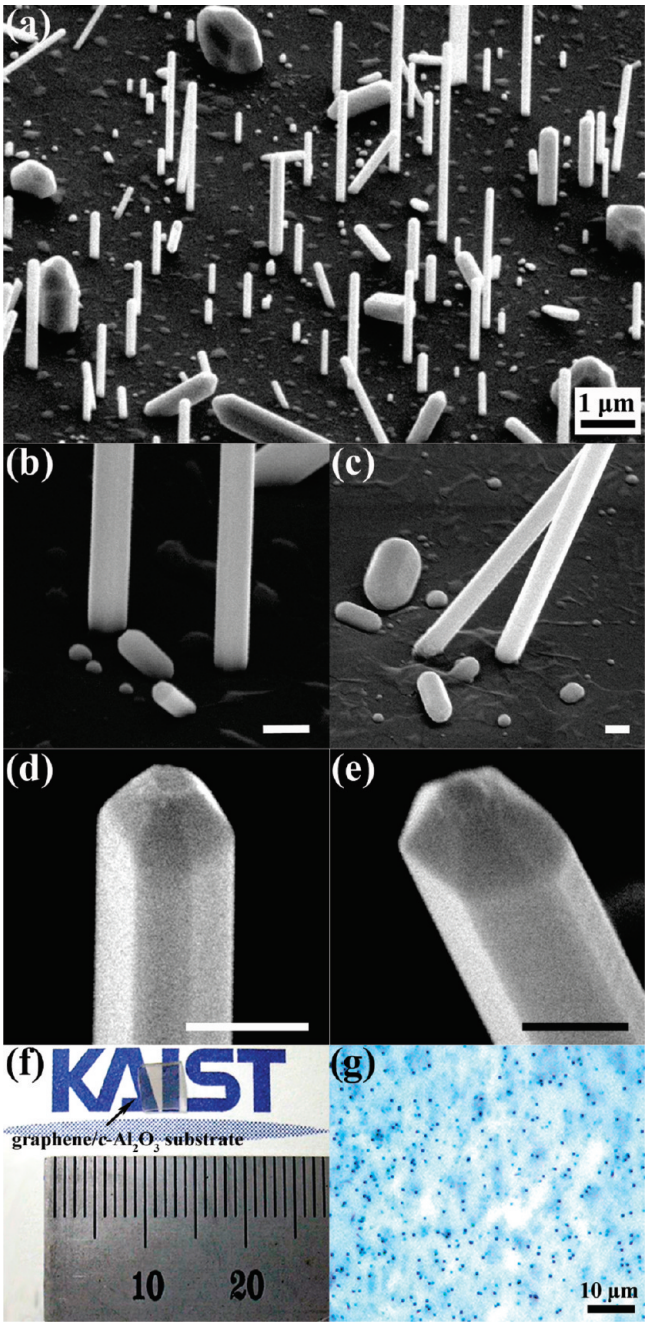

Figure 1. (a) Tilted-view SEM image of free-standing $Fe_{1.3}Ge$ NWs grown on a few-layer graphene/*c*-cut sapphire substrate. SEM images of (b) the vertical NW−graphene interface and (c) the inclined NW−graphene interface. High-magnification SEM images of (d) the vertical NW's tip and (e) the inclined NW's tip. The NWs have a hexagonal cross section along with a hexagonal pyramidal pointed tip (scale bars: 200 nm). Optical images of a graphene/*c*-cut sapphire substrate. (f) 5 × 5 mm^2 graphene on the sapphire substrate, showing that the film is transparent. (g) As-grown $Fe_{1.3}Ge$ NWs on the graphene/*c*-cut sapphire substrate. The numerous dark spots are from free-standing $Fe_{1.3}Ge$ NWs.

solid interface with graphene. Diameters of the NWs range from 150 to 250 nm and lengths up to ∼10 micrometers. The tips of vertical and inclined NWs have a hexagonal pyramidal shape (Figure 1d and e). An optical image of the graphene/*c*-cut sapphire (Figure 1f) shows that as-grown graphene is transparent. After synthesis, we observed a large number of black dark spots in the top view, which were as-grown vertical and inclined $Fe_{1.3}Ge$ NWs, as shown in Figure 1g. For the $Fe_{1.3}Ge$ NWs grown on a graphene/*c*-cut sapphire substrate, the density of $Fe_{1.3}Ge$ NWs is typically ∼50 NWs/100 μm^2. The ratio of vertical NWs to inclined NWs is about 7:3. From transmission electron microscope (TEM) and X-ray energy-dispersive spectrometry (EDS) analysis, as-synthesized NWs on graphene could be indexed to the hexagonal $Fe_{1.3}Ge$ (Figure S2, Supporting Information). We have recently reported ferromagnetic free-standing $Fe_{1.3}Ge$ NWs grown on a *c*-cut sapphire substrate.[21] In this study, we have successfully synthesized vertical $Fe_{1.3}Ge$ NWs on few-layer graphene.

If the $Fe_{1.3}Ge$ NWs were synthesized on a graphene/SiO_2/Si substrate, the NW−graphene integrated architecture could be easily separated from the SiO_2/Si substrate by etching the SiO_2 layer using a dilute HF solution. The NW−graphene structure then could be transferred onto other substrates for further applications. For this purpose, we have synthesized $Fe_{1.3}Ge$ NWs on a graphene/SiO_2/Si substrate of ∼5 × 5 mm^2 (Figure S3a, Supporting Information). Figure S3b (Supporting Information) displays a firm interface between $Fe_{1.3}Ge$ NWs and a graphene/SiO_2/Si substrate. The ratio of the vertical to inclined $Fe_{1.3}Ge$ NWs on this substrate was smaller than that for the graphene/*c*-cut sapphire. On the sapphire substrate and the SiO_2/Si substrate not covered by graphene, both inclined and horizontal NWs were synthesized (Figure S4, Supporting Information).

We performed a cross-section TEM analysis to investigate the interface between the vertical $Fe_{1.3}Ge$ NW and few-layer graphene (Figure 2a). For this study, a vertical cross section was sliced and thinned with a focused ion beam (FIB) technique.[28] To protect the underlying sample from ion beam damage during milling, the Pt layer was deposited over the area of interest using the FIB gas injection system prior to ion beam milling. The missing upper part of the vertical NW was a result of the ion milling during the sample preparation (Figure 2a). Figure 2b shows a high-resolution TEM (HRTEM) image of a $Fe_{1.3}Ge$ NW, a two-dimensional fast Fourier transform (FFT) (Figure 2c) of which could be indexed to the hexagonal $Fe_{1.3}Ge$ structure, indicating a [001] NW growth direction. The FFT pattern is recorded along the $[1\bar{1}0]$ zone axis. The HRTEM image of the vertical NW−graphene interface shows that the NW is directly integrated on the graphene (Figure 2b). The observed lattice planes of the $Fe_{1.3}Ge$ NW with a spacing of 0.20 and 0.25 nm (shown in Figure 2b) correspond to the (220) and (002) planes of hexagonal $Fe_{1.3}Ge$ (space group $P6_3/mmc$, JCPDS card no. 35-1182), respectively. For the few-layer graphene, observed spacing of 0.21 nm between the lattice planes is identical to that of the (100) planes of graphite. The lattice mismatch between $Fe_{1.3}Ge$ (220) and graphene (100) is less than 4.8%. The interlayer distance of the few-layer graphene is ∼0.36 nm, which is also close to 0.34 nm of graphite. The thickness of the few-layer graphene is estimated to be ∼2.7 nm in Figure 2b, corresponding to approximately eight graphene layers. EDS data (Figure 2d) on the NWs exhibit that only Fe and Ge are present in the NW in an average atomic ratio of 56:44. Cu peaks are from the TEM grid. However, we have also observed the NW synthesized on bi- or trilayer graphene, of which TEM images were difficult to obtain because the NWs were promptly damaged by the electron beam of the TEM. The vertical NW and graphene are interfaced by $Fe_{1.3}Ge(001)$ and graphene(001) planes. A schematic of atomic planes at the epitaxial interface (Figure 2e), viewed along the [001] direction of both $Fe_{1.3}Ge$ and graphene, shows that both the planes have a six-fold symmetry, and the lattice mismatch between the lattice spacing of

dx.doi.org/10.1021/jz2002925 |*J. Phys. Chem. Lett.* 2011, 2, 956–960

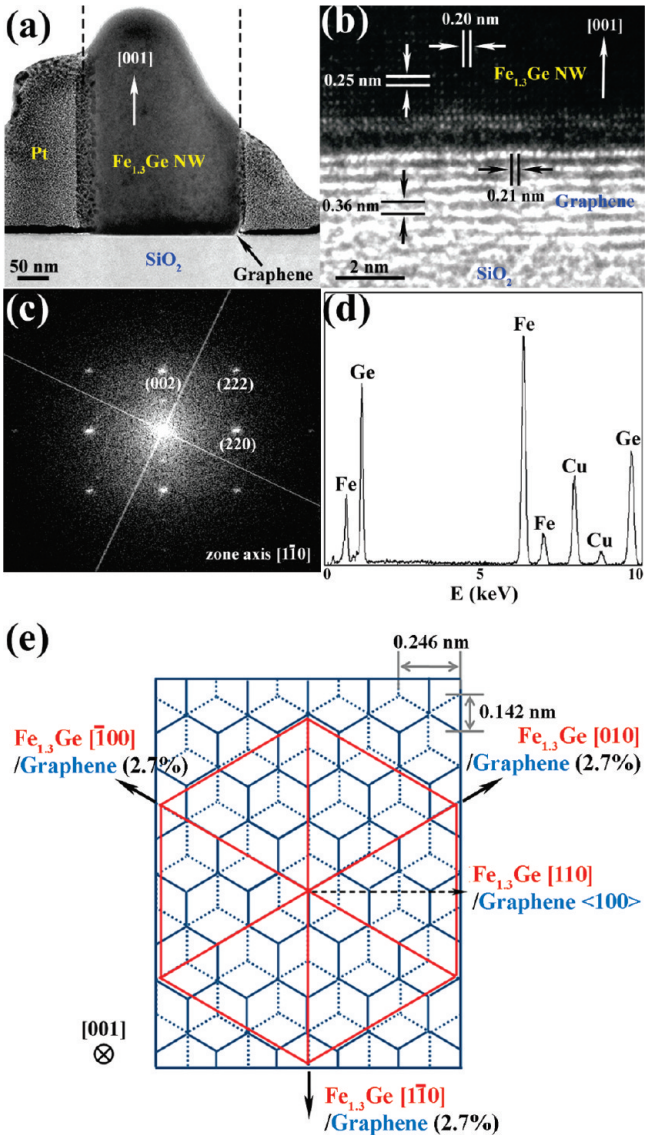

Figure 2. (a) A cross-section TEM image of the vertical $Fe_{1.3}Ge$ NW grown on few-layer graphene. (b) A cross-section HRTEM image of the interface between the NW and few-layer graphene, indicating that the vertical NW is directly integrated on the graphene without any gap or impurities between them. The thickness of the few-layer graphene is estimated to be ~2.7 nm, corresponding to approximately eight graphene layers. The lattice mismatch between the lattice spacing of $Fe_{1.3}Ge(220)$ planes (0.20 nm) and that of graphene(100) planes (0.21 nm) is apporximately 4.8%. (c) FFT obtaind from the HRTEM image in panel (b). The FFT pattern recorded along the [1$\bar{1}$0] zone axis can be indexed to the hexagonal $Fe_{1.3}Ge$ structure, indicating a [001] NW growth direction. (d) A TEM-EDS spectrum of a $Fe_{1.3}Ge$ NW reveals that Fe and Ge are the only elements present in the NW in an average atomic ratio of 56:44. (e) A schematic illustration of atomic planes at the epitaxial interface between the graphene and the $Fe_{1.3}Ge$ NW, viewed along the [001] direction of both $Fe_{1.3}Ge$ and graphene. The lattice spacing of $Fe_{1.3}Ge${100} planes (6.908 Å), perpendicular to the $Fe_{1.3}Ge$ (001), and the C−C nearest-neighbor distance in the hexagonal basal plane of graphene (1.42 Å) are related by a factor of 5, with a lattice mismatch as small as 2.7%.

$Fe_{1.3}Ge${100} planes (6.908 Å), perpendicular to the $Fe_{1.3}Ge$ (001), and the C−C nearest-neighbor distance in the hexagonal basal plane of graphene (1.42 Å) is as small as 2.7%. This suggests that epitaxial growth of $Fe_{1.3}Ge$ NWs on graphene that have a [001] growth direction can be ascribed to a good lattice match.

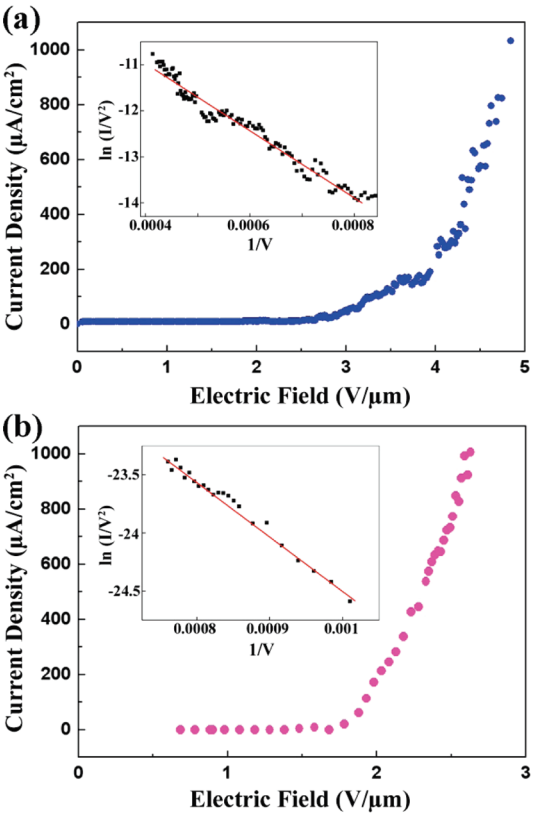

Figure 3. FE current density (J) versus applied electric field (E) measured on $Fe_{1.3}Ge$ NW arrays grown on (a) the graphene/c-cut sapphire substrate (after Au film coating) and (b) the HOPG substrate at a distance of 500 μm. Insets show a F−N plot obtained by plotting $\ln(I/V^2)$ versus $1/V$, which indicates that the emission behavior satisfies the F−N model, showing linear dependence.

The $Fe_{1.3}Ge$ NW−graphene/sapphire and the $Fe_{1.3}Ge$ NW−graphene/SiO_2/Si integrated structures thus synthesized did not show efficient field emission because good conduction was prevented by slight deformation of graphene imposed during the FE device fabrication process. To overcome this problem and improve the cathode conductivity, Au thin layers (<~7 nm) were deposited via metal evaporation onto a 3 × 4 mm^2 graphene/sapphire substrate on which $Fe_{1.3}Ge$ NWs were grown, and then, FE properties of the NWs were investigated. The NW−graphene/sapphire substrate coated with the Au thin film was used as a cathode panel. The J−E curve of the current density (J) versus applied electric field (E) is shown in Figure 3a. A turn-on voltage of 2.44 V μm^{-1} was obtained from the $Fe_{1.3}Ge$ NW arrays grown on the graphene/sapphire substrate after Au coating, and the emission current density of the NWs reached 1 mA cm^{-2} at an applied field of 4.84 V μm^{-1}. The turn-on voltage is defined as the applied electric field that produces a current density of 10 μA cm^{-2}. While this turn-on voltage is reasonably good compared to that of other nano-emitters,[29−32] it may not be the best performance that this $Fe_{1.3}Ge$ NW−graphene device can offer because the graphene cathode may have been partially damaged in contact regions between the graphene cathode and the FE equipment, leading to deteriorated conduction.

To alleviate the cathode damage, we have synthesized $Fe_{1.3}Ge$ NWs on a HOPG substrate, which is highly rigid and has a surface crystal structure identical to that of graphene. Figure S5

dx.doi.org/10.1021/jz2002925 |J. Phys. Chem. Lett. 2011, 2, 956–960

(Supporting Information) shows that vertical and inclined $Fe_{1.3}Ge$ NWs were synthesized similarly on HOPG as that on graphene. TEM measurements showed that the crystal structure, elemental composition, and growth direction of $Fe_{1.3}Ge$ NWs grown on HOPG were identical to those of NWs grown on graphene.

We have investigated FE properties of the free-standing $Fe_{1.3}Ge$ NW arrays grown on a 4×4 mm^2 HOPG substrate, which was used as a cathode panel. A $J-E$ curve is shown in Figure 3b. The turn-on voltage of the NW arrays grown on the HOPG was 1.58 V μm^{-1}, and the emission current density reached 1 mA cm^{-2} at an applied field of 2.63 V μm^{-1}. $J-E$ data obtained from multiple samples showed reproducible emission properties, while the bare HOPG and graphene did not show any FE. This turn-on voltage of the $Fe_{1.3}Ge$ NWs on HOPG, 1.58 V μm^{-1}, is quite low and approaches that of CNT arrays.[16,27] The $Fe_{1.3}Ge$ NWs on HOPG have shown more effective FE properties than those of the $Fe_{1.3}Ge$ NWs on graphene due to their stable conductive path. Thus, considerably better FE performance would be observed by forming an optimum contact in the graphene cathode. An improved device fabrication process is being explored to ensure good cathode conduction.

To understand the emission behavior, a Fowler–Nordheim (F–N) plot obtained by plotting $\ln(I/V^2)$ versus $1/V$ has been analyzed (insets in Figure 3). The plots could be fitted to a straight line, indicating that the emission satisfied the F–N tunneling mechanism.[16−18,29−32] From the slopes of the $\ln(I/V^2)-1/V$ plots and the work function value of $Fe_{1.3}Ge$, β values of the NWs grown on graphene and HOPG were calculated to be 4650 and 7300, respectively (Supporting Information). The β values of the NWs on graphene and HOPG are significantly higher than those of other NW emitters.[29−32] From these results, very efficient observed FE properties of $Fe_{1.3}Ge$ NWs grown on graphene and HOPG substrate can be ascribed to the well-interfaced vertical growth, a pointed tip shape, and the high β of the integrated NW arrays.

In conclusion, vertically aligned hexagonal $Fe_{1.3}Ge$ NWs have been successfully integrated on few-layer graphene in a large area as well as on HOPG. Vertical epitaxial growth of $Fe_{1.3}Ge$ NWs on graphene is ascribed to good lattice match. The $Fe_{1.3}Ge$ NW–graphene structure show efficient FE properties, suggesting application possibility as a future flexible field emission display. A well-interfaced vertical $Fe_{1.3}Ge$ NW–graphene integrated structure may open up further opportunities in the advanced nanoelectronics and nanospintronics.

EXPERIMENTAL METHODS

Growth of $Fe_{1.3}Ge$ NWs. $Fe_{1.3}Ge$ NW arrays were synthesized on both a few-layer graphene film and a HOPG substrate in a hot wall two-zone furnace by using a CVT process. The furnace contains a 1 in. diameter quartz tube. As a Fe precursor, anhydrous FeI_2 powder (Sigma-Aldrich, 99.99%) in an alumina boat was placed at the center of the upstream (US) zone. The substrates were placed on an alumina boat filled up with a powdered Ge/C mixture of 1:1 (weight ratio) Ge powder (Sigma-Aldrich, 99.999%) and graphite powder (Kanto chemical Co.), which were placed ~18 cm away from the FeI_2 in the downstream (DS) zone. The DS zone was initially heated to 870 °C. The US zone heating started when the DS zone reached 700 °C. After the US zone reached 650 °C, the reaction was maintained for 10 min at the temperature. An Ar flow rate of ~200 sccm and pressure of 1 atm were maintained during the reaction.

Graphene Preparation. Centimeter-scale graphene layers were grown on Ni-coated SiO_2/Si substrates through the use of chemical vapor deposition (CVD) by using methane (CH_4) as a carbon source under a H_2 and Ar atmosphere at 1000 °C, as we reported in a previous paper.[12] As-grown graphene layers were then detached from the substrates by subsequent etching of the SiO_2 and Ni layers underneath of the graphene with an aqueous hydrogen fluoride (HF) and Ni etchant, respectively. Due to the hydrophobic surface of graphene layers, the free-standing graphene layers were floated on an aqueous solution and could be mounted on an arbitrary substrate such as a *c*-cut sapphire and SiO_2/Si. To exclude the effect of the Ni as a catalyst on the $Fe_{1.3}Ge$ NW growth, we employed the free-standing graphene film. The entire surface of the sapphire and SiO_2/Si substrates was covered with the free-standing graphene film, and the size of the transferred graphene film was dependent on that of the substrates, although centimeter-scale graphene films can be synthesized via the use of CVD.

Characterization. FE-SEM images of hexagonal $Fe_{1.3}Ge$ NWs were taken on a Phillips XL30S. TEM and HRTEM images and SAED patterns were taken on a JEOL JEM-2100F TEM operated at 200 kV. Compositions of the $Fe_{1.3}Ge$ NWs were studied by EDS. The electron FE of hexagonal $Fe_{1.3}Ge$ NWs grown on a HOPG substrate and graphene in a vacuum of 2×10^{-6} Torr was measured by applying a DC voltage across 500 μm between an anode and a cathode.

ASSOCIATED CONTENT

Supporting Information. Identification data of the as-grown graphene film and additional SEM, TEM, and FE data of $Fe_{1.3}Ge$ NWs. This material is available free of charge via the Internet at http://pubs.acs.org.

AUTHOR INFORMATION

Corresponding Author

*E-mail: bongsoo@kaist.ac.kr. Fax: +82-42-350-2810.

ACKNOWLEDGMENT

This research was supported by KOSEF through NRL (2010-0018868), SRC (2011-0001335), and "Center for Nanostructured Material Technology" under the "21st Century Frontier R&D Programs" (2010-K000350) of the MEST, Korea. SEM and TEM analyses were performed at the KBSI in Daejeon.

REFERENCES

(1) Liao, L.; Lin, Y. C.; Bao, M.; Cheng, R.; Bai, J.; Liu, Y.; Qu, Y.; Wang, K. L.; Huang, Y.; Duan, X. High-Speed Graphene Transistors with a Self-Aligned Nanowire Gate. *Nature* **2010**, *467*, 305–308.

(2) Avouris, P. Graphene: Electronic and Photonic Properties and Devices. *Nano Lett.* **2010**, *10*, 4285–4294.

(3) Kim, K. S.; Zhao, Y.; Jang, H.; Lee, S. Y.; Kim, J. M.; Kim, K. S.; Ahn, J. H.; Kim, P.; Choi, J. Y.; Hong, B. H. Large-Scale Pattern Growth of Graphene Films for Stretchable Transparent Electrodes. *Nature* **2009**, *457*, 706–710.

(4) Wang, R.; Hao, Y.; Wang, Z.; Gong, H.; Thong, J. T. L. Large-Diameter Graphene Nanotubes Synthesized Using Ni Nanowire Templates. *Nano Lett.* **2010**, *10*, 4844–4850.

(5) Wang, X.; Zhi, L.; Müllen, K. Transparent, Conductive Graphene Electrodes for Dye-Sensitized Solar Cells. *Nano Lett.* **2008**, *8*, 323–327.
(6) Hong, T. K.; Lee, D. W.; Choi, H. J.; Shin, H. S.; Kim, B. S. Transparent, Flexible Conducting Hybrid Multilayer Thin Films of Multiwalled Carbon Nanotubes with Graphene Nanosheets. *ACS Nano* **2010**, *4*, 3861–3868.
(7) Cote, L. J.; Kim, F.; Huang, J. Langmuir−Blodgett Assembly of Graphite Oxide Single Layers. *J. Am. Chem. Soc.* **2009**, *131*, 1043–1049.
(8) Tombros, N.; Jozsa, C.; Popinciuc, M.; Jonkman, H. T.; Van Wees, B. J. Electronic Spin Transport and Spin Precession in Single Graphene Layers at Room Temperature. *Nature* **2007**, *448*, 571–574.
(9) Eom, D.; Prezzi, D.; Rim, K. T.; Zhou, H.; Lefenfeld, M.; Xiao, S.; Nuckolls, C.; Hybertsen, M. S.; Heinz, T. F.; Flynn, G. W. Structure and Electronic Properties of Graphene Nanoislands on Co(0001). *Nano Lett.* **2009**, *9*, 2844–2848.
(10) Goto, H.; Kanda, A.; Sato, T.; Tanaka, S.; Ootuka, Y.; Odaka, S.; Miyazaki, H.; Tsukagoshi, K.; Aoyagi, Y. Gate Control of Spin Transport in Multilayer Graphene. *Appl. Phys. Lett.* **2008**, *92*, 212110/1–212110/3.
(11) Liao, L.; Bai, J.; Cheng, R.; Lin, Y. −C.; Jiang, S.; Huang, Y.; Duan, X. Top-Gated Graphene Nanoribbon Transistors with Ultrathin High-*k* Dielectrics. *Nano Lett.* **2010**, *10*, 1917–1921.
(12) Lee, J. M.; Pyun, Y. B.; Yi, J.; Choung, J. W.; Park, W. I. ZnO Nanorod−Graphene Hybrid Architectures for Multifunctional Conductors. *J. Phys. Chem. C* **2009**, *113*, 19134–19138.
(13) Lee, J. M.; Choung, J. W.; Yi, J.; Lee, D. H.; Samal, M.; Yi, D. K.; Lee, C. H.; Yi, G. C.; Paik, U.; Rogers, J. A.; Park, W. I. Vertical Pillar−Superlattice Array and Graphene Hybrid Light Emitting Diodes. *Nano Lett.* **2010**, *10*, 2783–2788.
(14) Chung, K.; Lee, C. H.; Yi, G. C. Transferable GaN Layers Grown on ZnO-Coated Graphene Layers for Optoelectronic Devices. *Science* **2010**, *330*, 655–657.
(15) Kim, Y. K.; Na, H. K.; Lee, Y. W.; Jang, H.; Han, S. W.; Min, D. H. The Direct Growth of Gold Rods on Graphene Thin Films. *Chem. Commun.* **2010**, *46*, 3185–3187.
(16) Lee, D. H.; Lee, J. A.; Lee, W. J.; Kim, S. O. Flexible Field Emission of Nitrogen-Doped Carbon Nanotubes/Reduced Graphene Hybrid Films. *Small* **2010**, *7*, 95–100.
(17) Hwang, J. O.; Lee, D. H.; Kim, J. Y.; Han, T. H.; Kim, B. H.; Park, M.; No, K.; Kim, S. O. Vertical ZnO Nanowires/Graphene Hybrids for Transparent and Flexible Field Emission. *J. Mater. Chem.* **2011**, *21*, 3432–3437.
(18) Yoon, H.; Seo, K.; Bagkar, N.; In, J.; Park, J.; Kim, J.; Kim, B. Vertical Epitaxial Co_5Ge_7 Nanowire and Nanobelt Arrays on a Thin Graphitic Layer for Flexible Field Emission Displays. *Adv. Mater.* **2009**, *21*, 4979–4982.
(19) Shang, N.; Papakonstantinou, P.; Wang, P.; Silva, S. R. P. Platinum Integrated Graphene for Methanol Fuel Cells. *J. Phys. Chem. C* **2010**, *114*, 15837–15841.
(20) Wang, H.; Cui, L. F.; Yang, Y.; Casalongue, H. S.; Robinson, J. T.; Liang, Y.; Cui, Y.; Dai, H. Mn_3O_4−Graphene Hybrid as a High-Capacity Anode Material for Lithium Ion Batteries. *J. Am. Chem. Soc.* **2010**, *132*, 13978–13980.
(21) Yoon, H.; Lee, A. T.; Choi, E. A.; Seo, K.; Bagkar, N.; Cho, J.; Jo, Y.; Chang, K. J.; Kim, B. Structure-Induced Ferromagnetic Stabilization in Free-Standing Hexagonal $Fe_{1.3}Ge$ Nanowires. *J. Am. Chem. Soc.* **2010**, *132*, 17447–17451.
(22) Gaudet, S.; Detavernier, C.; Kellock, A. J.; Desjardins, P.; Lavoie, C. Thin Film Reaction of Transition Metals with Germanium. *J. Vac. Sci. Technol. A* **2006**, *24*, 474–485.
(23) Massenet, O.; Daver, H.; Geneste, J. Magnetic Ordering and Magnetization in Amorphous Fe−Ge Films. *J. Phys. Colloq.* **1974**, *35*, C4/279–C4/285.
(24) Tang, J.; Wang, C. Y.; Xiu, F.; Hong, A. J.; Chen, S.; Wang, M.; Zeng, C.; Yang, H. J.; Tuan, H. Y.; Tsai, C. J.; Chen, L. J.; Wang, K. L. Single-Crystalline Ni_2Ge/Ge/Ni_2Ge Nanowire Heterostructure Transistors. *Nanotechnology* **2010**, *21*, 505704/1–505704/7.
(25) van der Meulen, M. I.; Petkov, N.; Morris, M. A.; Kazakova, O.; Han, X.; Wang, K. L.; Jacob, A. P.; Holmes, J. D. Single Crystalline $Ge_{1-x}Mn_x$ Nanowires as Building Blocks for Nanoelectronics. *Nano Lett.* **2009**, *9*, 50–56.
(26) Maassen, J.; Ji, W.; Guo, H. Graphene Spintronics: The Role of Ferromagnetic Electrodes. *Nano Lett.* **2011**, *11*, 151–155.
(27) Cho, Y.; Kim, C.; Moon, H.; Choi, Y.; Park, S.; Lee, C. K.; Han, S. Electronic Structure Tailoring and Selective Adsorption Mechanism of Metal-Coated Nanotubes. *Nano Lett.* **2008**, *8*, 81–86.
(28) Liu, Z.; Elbert, D.; Chien, C. L.; Searson, P. C. FIB/TEM Characterization of The Composition and Structure of Core/Shell Cu−Ni Nanowires. *Nano Lett.* **2008**, *8*, 2166–2170.
(29) Yoon, H.; Seo, K.; Moon, H.; Varadwaj, K. S. K.; In, J.; Kim, B. Aluminum Foil Mediated Noncatalytic Growth of ZnO Nanowire Arrays on an Indium Tin Oxide Substrate. *J. Phys. Chem. C* **2008**, *112*, 9181–9185.
(30) Li, L.; Fang, X.; Chew, H. G.; Zheng, F.; Liew, T. H.; Xu, X.; Zhang, Y.; Pan, S.; Li, G.; Zhang, L. Crystallinity-Controlled Germanium Nanowire Arrays: Potential Field Emitters. *Adv. Funct. Mater.* **2008**, *18*, 1080–1088.
(31) Ok, Y. W.; Seong, T. Y.; Choi, C. J.; Tu, K. N. Field Emission from Ni-Disilicide Nanorods Formed by Using Implantation of Ni in Si Coupled with Laser Annealing. *Appl. Phys. Lett.* **2006**, *88*, 043106/1–043106/3.
(32) Li, L.; Xu, X.; Chew, H.; Huang, X.; Dou, X.; Pan, S.; Li, G.; Zhang, L. Direct Growth of Al Nanowire Arrays: Thermal Expansion and Field Emission Properties. *J. Phys. Chem. C* **2008**, *112*, 5328–5332.